Visualization methods for understanding the dynamic electroadhesion phenomenon

BAMBER, T, GUO, J, SINGH, J, BIGHARAZ, Masoud, PETZING, J, BINGHAM, Paul <http://orcid.org/0000-0001-6017-0798>, JUSTHAM, L, PENDERS, Jacques <http://orcid.org/0000-0002-6049-508X> and JACKSON, M

Published version

BAMBER, T, GUO, J, SINGH, J, BIGHARAZ, Masoud, PETZING, J, BINGHAM, Paul, JUSTHAM, L, PENDERS, Jacques and JACKSON, M (2017). Visualization methods for understanding the dynamic electroadhesion phenomenon. Journal of Physics D: Applied Physics, 50, p. 205304.

Visualization methods for understanding the dynamic electroadhesion phenomenon

2017 J. Phys. D: Appl. Phys. 50 205304

OPEN ACCESS
IOP Publishing
Journal of Physics D: Applied Physics
J. Phys. D: Appl. Phys. **50** (2017) 205304 (8pp)
https://doi.org/10.1088/1361-6463/aa6be4

Visualization methods for understanding the dynamic electroadhesion phenomenon

T Bamber[1,3], J Guo[1,3], J Singh[2], M Bigharaz[2], J Petzing[1], P A Bingham[2], L Justham[1], J Penders[2] and M Jackson[1]

[1] EPSRC Centre for Innovative Manufacturing in Intelligent Automation, Wolfson School of Mechanical, Electrical and Manufacturing Engineering, Loughborough University, Loughborough, Leicestershire LE11 3TU, United Kingdom
[2] Materials and Engineering Research Institute, Sheffield Hallam University, City Campus, Howard Street, Sheffield S1 1WB, United Kingdom

E-mail: J.Guo@lboro.ac.uk

Received 24 October 2016, revised 5 April 2017
Accepted for publication 6 April 2017
Published 26 April 2017

Abstract

Experimental investigation into the surface potential and electric field visualization of an electroadhesion system is presented for understanding the dynamic electroadhesion phenomenon. The indirect experimental approach has been based on measuring surface potentials on the surface of an electroadhesive pad by an electrostatic voltmeter. The direct approach has been based on charging and discharging the electroadhesive pad in a viscous oil mixed with lightweight particles. The visualization of the dynamic field distribution of electroadhesive pads can be a useful method to understand the dynamic electroadhesion phenomenon. In addition, indication of different field distributions of different pad geometries can be obtained through the method demonstrated here. Furthermore, the method is useful for instructors or lecturers to showcase or teach the dynamic electroadhesion phenomenon.

Keywords: electroadhesion, field visualization, surface potential measurement, dynamic electrostatic field distribution

S Supplementary material for this article is available online

(Some figures may appear in colour only in the online journal)

1. Introduction

Electroadhesion [1, 2] is an electrically controllable attractive effect between an electroadhesive pad and a substrate. Electroadhesion has been considered as an advanced adhesion mechanism for robots such as climbing robots [3] and a range of material handling applications [4, 5]. Compared to other adhesion mechanisms for handling materials, such as magnetic adhesion, pneumatic adhesion, bioinspired adhesion, and mechanical gripping mechanisms [6], electroadhesion has several distinctive advantages including that: (1) it enables an enhanced adaptability as it can be used in vacuum environments and adheres to both conductive and insulating surfaces; (2) it can bring lightweight and reduced complexity systems as pumps or motors are not required for the end effector actuation; (3) it features low-noisy, flexible, and gentle handling characteristics as non-contact suspension mechanisms and soft-contact mechanisms can be applied to produce non-damaging or less-damaging grasping systems; (4) it is an ultra-low energy consumption adhesion method as a small current, in the μA to mA range, runs through the electroadhesive pad, resulting a small energy consumption, usually in the μW to mW range [5, 7].

An electroadhesion system usually contains four main components: an electroadhesive pad, a high voltage power supply, a control system, and a substrate. The substrate is the material to which electroadhesion is applied, or a wall to hold

[3] Both authors contributed equally to this work.

on, or a piece of material to be picked. An electroadhesive pad typically consists of conductive electrodes embedded in one or more dielectric materials [8]. The conductive electrodes are connected with one or more high voltage sources, usually in the kV range. The dielectric material is useful for preventing charge neutralization and dielectric breakdown of the pad. The control system manages switching on and off the electroadhesion system [8].

Electroadhesion is a complex and dynamic electrostatically induced attraction phenomenon with over 33 variables, including environmental factors, electrode parameters, pad dielectric parameters, substrate parameters, and voltage parameters [4, 9], influencing the electroadhesive forces obtainable between the electroadhesive pad and the substrate. One limitation of electroadhesion is that the electroadhesive forces obtainable may be unstable and unpredictable in a changing environment [8, 9]. Also, not all substrate materials are suitable for electroadhesive force generation [10, 11]. Both the electroadhesive clamping and de-clamping process have a dynamic nature, which is an additional limitation since at the start, when turning on the power source the electroadhesive force does not reach the maximum magnitude immediately. Also, when disconnecting the power supply the adhesion does not stop immediately and residual charges and hence residual adhesive forces remain for a period. Force against time is depicted in figure 1.

As shown in figure 1, when the electroadhesive pad is energized by the high voltage sources ($t = t_0$), the electroadhesive force does not increase to its maximum magnitude immediately. Within a certain period ($t = t_1$), the electroadhesive force increases to a magnitude ($F = F_1$) that is slightly less than the maximum force ($F = F_{\text{saturated}}$). The time (t_1) may range from seconds to minutes. When the pad is placed on some semi-conductive and conductive materials, t_1 is of the order of seconds [3]. When the pad is placed on some insulating materials the time t_1 can be minutes or hours. For example, as can be seen in figure 2, at least 3 min of clamping time has been recorded when the polyimide side of an electroadhesive pad had been attached to a sheet of glass (the particular setup of this experiment has been described in Guo *et al* [4].). From F_1 to the maximum magnitude ($F = F_{\text{saturated}}$), the time can be relatively long, depending the electroadhesion property of the pad dielectric material and the substrate. When the pad is turned off the electroadhesive force does not disappear immediately. The de-clamping time can be fast if novel methods are employed such as exponentially decreasing reversion of the polarity [12]. If not, the de-clamping time can, however, be hours, as can be seen in figure 2. The examples of the variation in clamping and de-clamping times show the influence of materials used and their properties on the electroadhesive process, but these are just a few of the influencing variables. Normally an electroadhesive pad consists of two electrodes, one positive and one negative. However for industrial applications an extended gripping surface is required to generate the appropriate gripping force, which poses questions about the geometrical design of such extended pads. The aim of the current paper is to aid the understanding of the dynamic

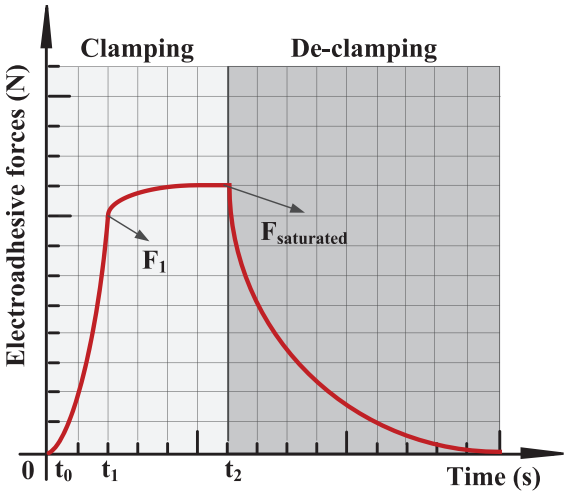

Figure 1. Schematic diagram of the dynamic electroadhesive clamping and de-clamping process.

electroadhesion phenomenon in particular for the pick-up and release performance of electroadhesive material handling applications such as the handling of copper laminates, paper, or polyimide plates, among others [8].

At present, in the electroadhesion community, the dynamic electroadhesive clamping and de-clamping process has only been characterized by measuring forces between the pad and substrate [4, 13]. This method, however, cannot provide a visualization of the dynamic electric field changing process nor does it show the electric field and charge distribution induced by the electroadhesive pad. Visualization of the dynamic electric field or charge distribution is a useful alternative method to understand, apply and optimize the dynamic electroadhesion phenomenon. In addition, indications of different field distributions of different pad geometries can be obtained. Furthermore, visualization is also useful for demonstrators or lecturers to showcase the dynamic electrostatic field distribution of the dynamic electroadhesion phenomenon.

Two field visualization methods for understanding the dynamic electroadhesion phenomenon have been presented in this paper. The visualization methods have been implemented using an indirect and direct approach. Although no specific dynamic field visualization work has been conducted concerning electroadhesion, others have used fluid based field visualization method to understand the dynamic pattern formation process of charged particles [14] and AC electrokinetics [15]. The direct field visualization approach presented in this paper has been inspired by these. The indirect experimental approach, as described in section 2, has been based on measuring surface potentials on an electroadhesive pad using a commercial electrostatic voltmeter. The direct approach, as described in section 3, has been based on charging and discharging the electroadhesive pad when it is submerged in sunflower oil mixed with semolina, i.e. lightweight solid particles suspended in a viscous medium. The focus of this paper has been on understanding the charging/clamping phase of the electroadhesion phenomenon. Finally, the conclusions and future work are summarized in section 4.

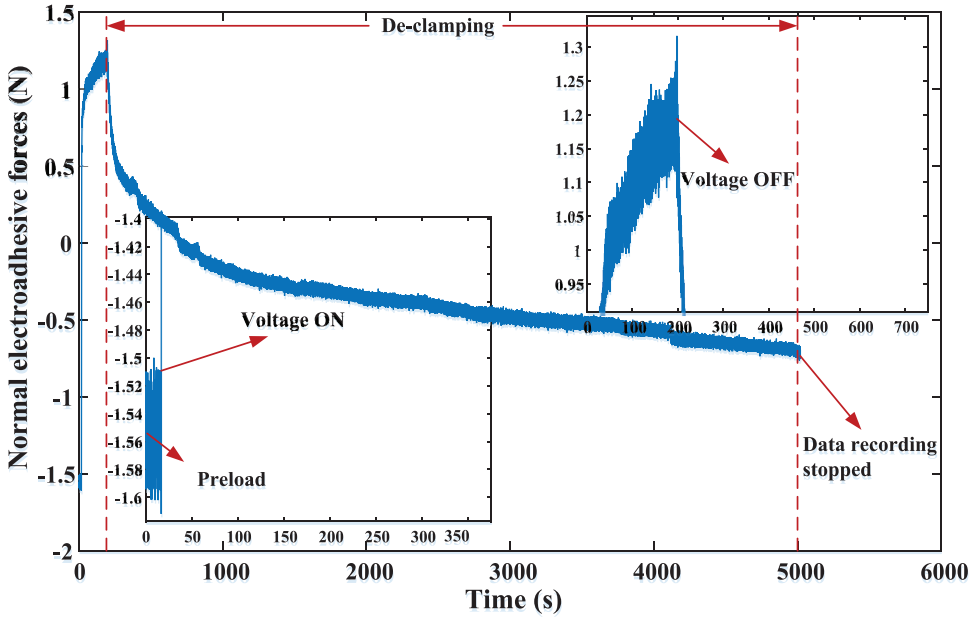

Figure 2. An example of the dynamic electroadhesive clamping and de-clamping process.

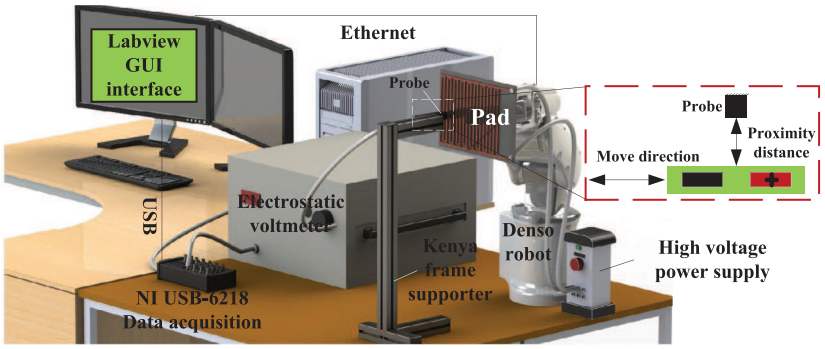

Figure 3. System diagram of the experiment setup for surface potential distribution visualization.

2. Surface potential visualization of the electroadhesion phenomenon

2.1. Experimental setup

The electric field is the gradient of the potential field based on the Maxwell equation. The potential field distribution on the surface of an electroadhesive pad can be measured by an electrostatic voltmeter.

The experimental setup to visualize the surface potential distribution of the electroadhesive pad is shown in figure 3, where a commercial non-contact electrostatic voltmeter (TREK, Inc.) has been used. The non-contact electrostatic voltmeter employs a field-nulling technique to capture the potential field and ensures accurate measurement not only for stationary surfaces but also for moving surfaces [16]. The sensing probe, connected with the voltmeter, has been fixed on a Kenya frame to measure the surface potentials on the electroadhesive pad. The recommended probe-to-surface separation distance is 3 mm ± 1 mm [15]. The proximity distance variability test has also shown that different proximity distances (2 mm, 3 mm, and 4 mm) generate similar results. The proximity distance has, therefore, been fixed here at 2 mm. The probe has been earthed before the start of the experiments using an earthed metal plate. A specific probe holder has been designed following the instructions from reference [16]. The holder has been specifically insulated using a polyethylene self-amalgamating tape (RS Components, Ltd) which has a 34 kV mm^{-1} breakdown voltage [17], as shown in figure 5. To minimize the error introduced by electrostatic induction the side view probe has been placed perpendicular to the surface instead of being parallel to the surface. The sampling rate of the data acquisition card, NI USB-6218, connected with the PC Labview, has been fixed at 20 Hz.

The electroadhesive pad used in this indirect field measurement approach has been based on an interdigital design, with electrode width of 4 mm, spacing between electrodes of 9.3 mm, and effective pad area of 190 mm × 230 mm (see figure 5). The pad has been made in-house based on a cost-effective pad design and manufacturing process [18]. The electrodes were made of copper. The dielectric covering the electrodes was polyurethane, which was the pad side facing the probe. The pad has been energised by a mono-polar ETH DC power supply from Unilab. The power source has

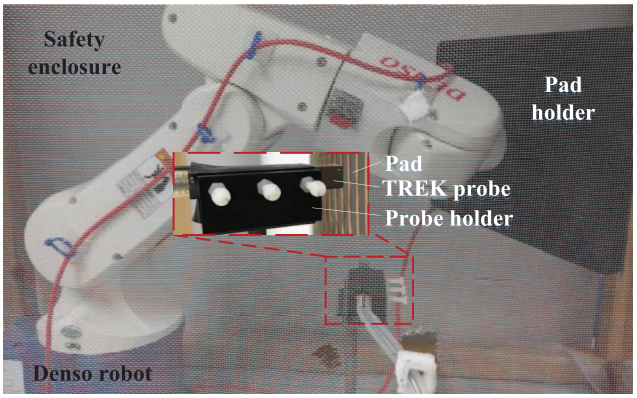

Figure 4. Physical setup for surface potential distribution visualization.

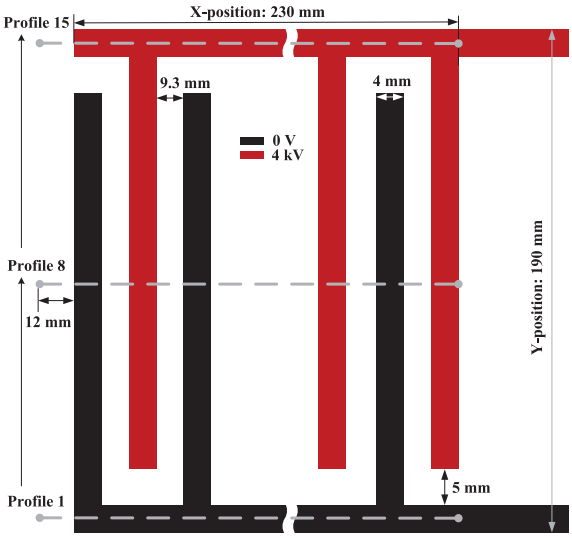

Figure 5. Electroadhesive pad design.

an output of 0–5 kV and a low current output value of 2 mA (maximum). 4 kV has been applied to the pad (see the red electrode in figure 5). The electroadhesive pad has been fixed onto the pad holder of a Denso robot (see figure 4). The robot has been driven to move backward and forward and 15 profiles or scan locations, as shown in figure 5, have been selected on the pad for the measurements. The starting point of the surface potential measurement on the pad was 12 mm before the first left electrode. The profile length was 242 mm.

2.2. Experimental procedure and results

The robot speed variability test, based on the profile 8 on the pad (figure 5), has shown that different movement speeds would generate close results, as demonstrated in figure 6. The speed of the movement has been fixed at 1 mm s^{-1}. It can be seen from figure 6 that different trends were obtained on the edge electrodes, compared to the middle electrodes. This is due to the fact that the voltage applied to the first electrode was 0 V and the last electrode was 4 kV.

The experimental procedure for each of the 15 profiles starts with turning on the pad. Taking the profile 8 as an

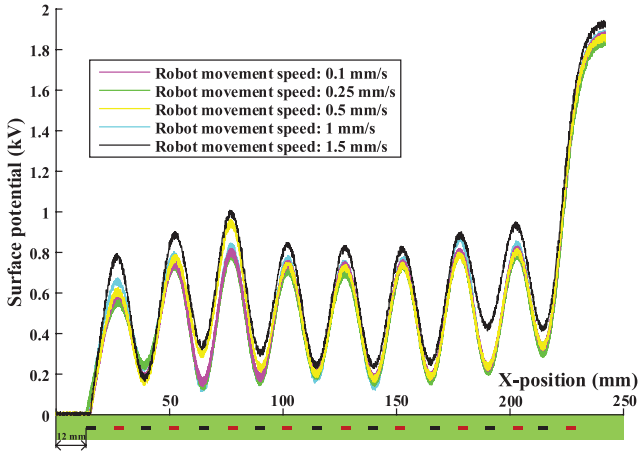

Figure 6. Movement speed variability test result based on the profile 8 (central profile) of the pad.

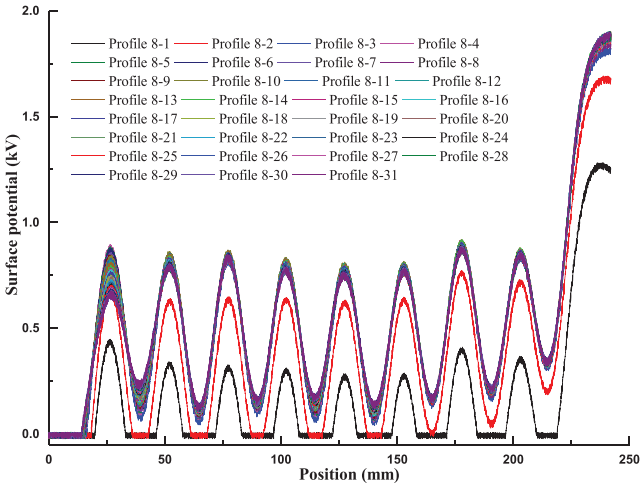

Figure 7. Surface potential results of the 4 h charging of the pad based on the profile 8.

example, over a period of 4 h, the robot moves the pad forward and backward, with the speed of 1 mm s^{-1}, to obtain the surface potential distribution. As can be seen from figure 7, in total 31 different surface potential distributions of the profile 8 can therefore be obtained, manifesting and proving that the charging period of the pad is indeed a dynamic process. Also, during the pad saturation period, there is little difference between the surface potential distribution results of the forward and backward movement. The very high measured potential of the electrode with the highest x-position (shown in figures 6–8) is due to this electrode being positively biased, and with no negative electrode on the far side. This result can therefore be explained and does not impact on any of the other results or the conclusions we are able to draw from this work.

Only the last surface potential distribution of each profile has been selected. The surface potential distribution of the pad after the pad saturation, based on the 15 profiles, is demonstrated in figure 8. This is useful for indicating the surface potential distribution of the electroadhesive pad. In addition, the result is useful for empirical modelling of the dynamic electroadhesion phenomenon.

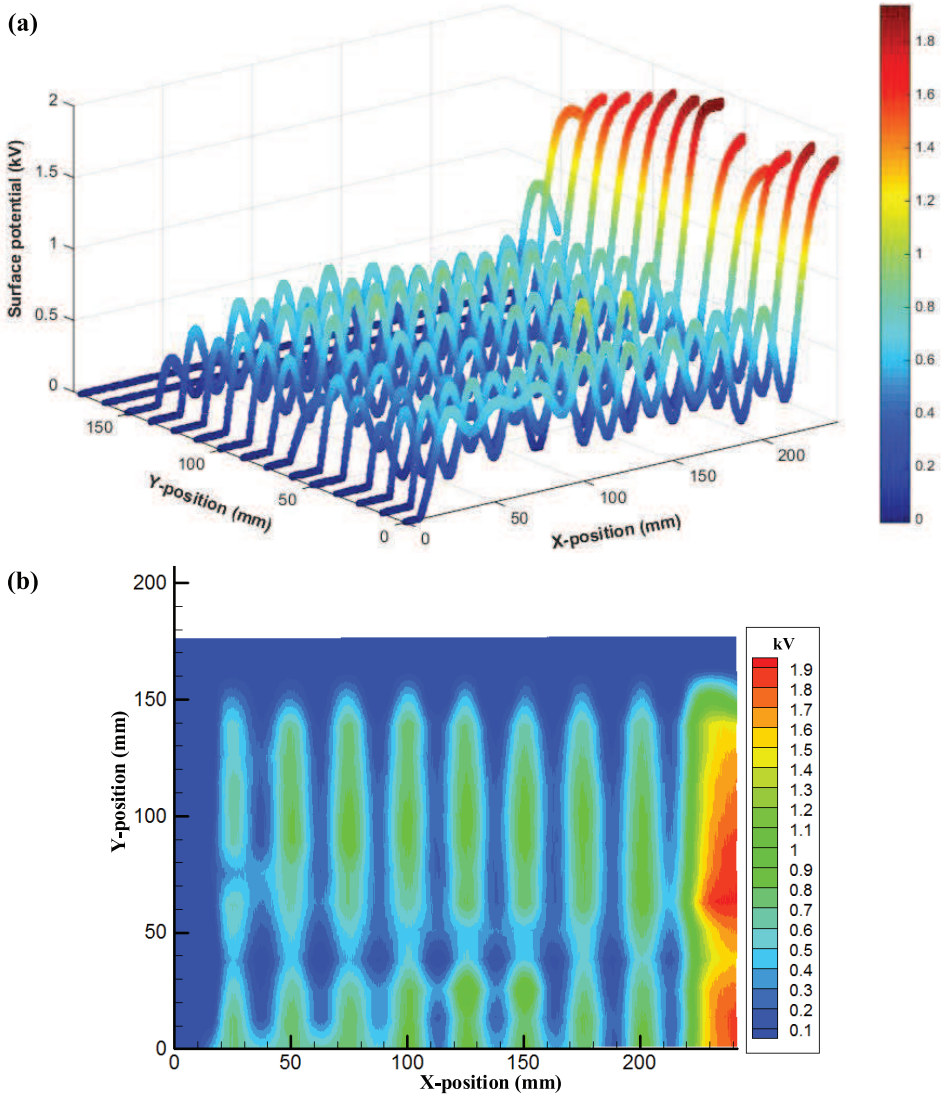

Figure 8. Surface potential distribution of the pad after the pad saturation: (a) 3D view and (b) contour plot.

3. Electric field visualization of the electroadhesion phenomenon

3.1. Experimental setup

A low-cost and effective experimental setup has been designed and implemented to visualize the dynamic electric field distribution of the dynamic electroadhesion phenomenon, as shown in figure 9.

This setup has been based on a 640 × 480, 250 frame per second (fps) high speed camera viewing the dynamic electric field distribution of the same pad used in section 2. The pad has been submerged in a container filled with semolina particles and sunflower oils. The semolina particles provide a low-density solid which is suspended in the viscous oil medium, providing the contrast necessary for visualizing the dynamic electric field. The semolina particles and sunflower oils have been mixed evenly before each experiment. The pad has been charged under potential difference of 4 kV based on one positive and negative EMCO high voltage converter (HVC). The EMCO HVC has an output from 0 V to 10 kV, with a reference input from 0 V to 5 V provided by a DC power supply unit (PSU).

3.2. Results and discussion

It can be seen from figures 10(a)–(f) that the electric field distribution during the charging process of the pad is shown to be dynamic, which is illustrated by the dynamic alignment of the particles throughout the recording between the positive electrodes on the left and the negative electrodes on the right.

The semolina particles have been uniformly spread throughout the oil and a general haze can be seen in figure 10(a) before turning on the voltage. After turning on the voltage, the dynamic fields are shown to cause motion in the oil/semolina mixture, as demonstrated in figure 10(b). This wave motion has caused the reflection from the lighting source into the camera and at this point the particles have not started to align strongly. The particles have begun to clearly align with each other between the positive and negative electrodes, as shown in figures 10(c)–(e), before the settlement of this dynamic process, as shown in figure 10(f), where curved field distribution concentrations can be seen at the corners.

A 2D COMSOL electrostatic simulation of the electroadhesive pad has been conducted to compare the stable experiment electric distribution and with the electrostatic

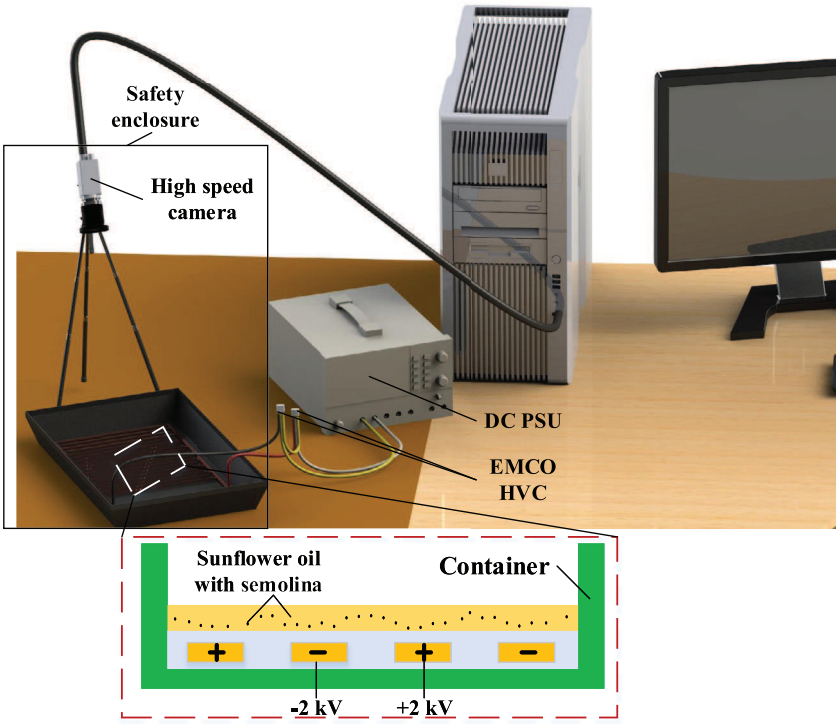

Figure 9. Experimental setup for electric field distribution visualization of the pad.

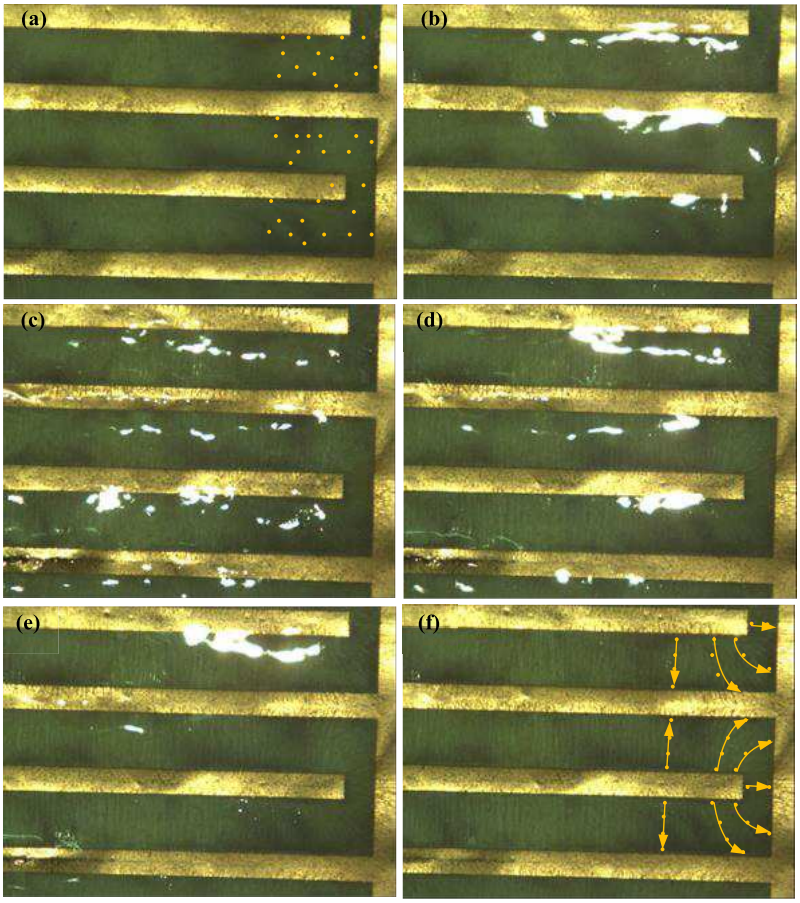

Figure 10. Dynamic electric distribution during the charging process of the electroadhesive pad when: (a) $t = 0$ s, (b) $t = 0.15$ s, (c) $t = 0.5$ s, (d) $t = 1$ s, (e) $t = 1.5$ s, (f) $t = 3$ s. Yellow dots and arrows highlight starting positions and movement/alignment of semolina particles. Arrows shown in (f) indicate the steady alignment of the particles after applying the electric field for 3 s. A clearer view of this dynamic process can be seen in the supplementary video (stacks.iop.org/JPhysD/50/205304/mmedia).

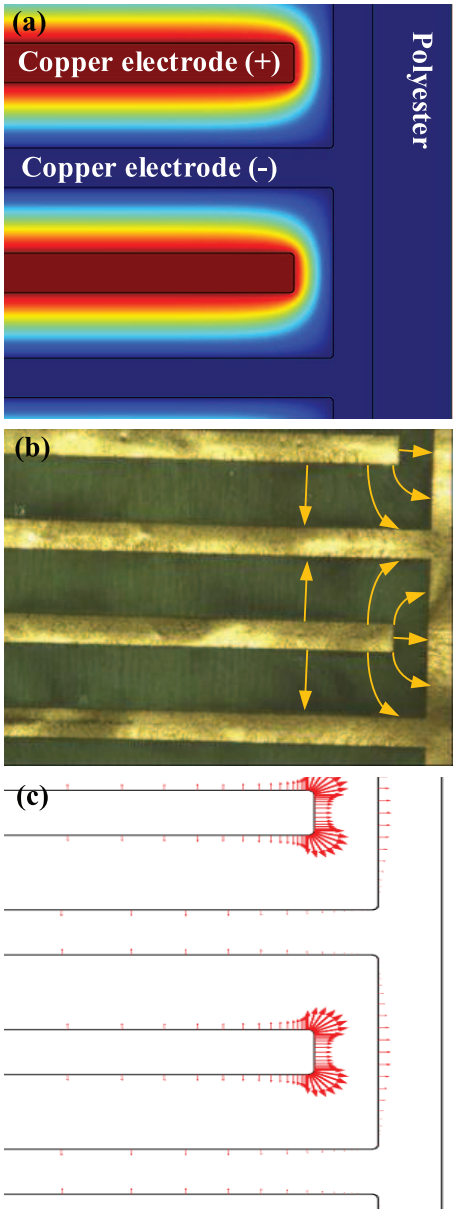

Figure 11. Comparison between the stable experiment electric distribution and the electrostatic distribution of the electroadhesive pad: (a) sectional electric potential distribution of the 2D COMSOL electrostatic model of the pad, (b) sectional stable experiment electric field distribution of the pad (yellow arrows show alignment of semolina particles), and (c) sectional 2D COMSOL static electric field distribution of the pad, where the length of the arrows was proportional to the electric field strength.

distribution of the corner part of the pad. The materials used in the 2D electrostatic simulation were also copper and polyester (dielectric constant of 3), as shown in figure 11(a). The electrode dimensions were the same with the parameters demonstrated in figure 6. The dimension of the polyester in the simulation was 210 mm × 297 mm. The Electrostatic module was used for this study and finer physically-controlled mesh was applied. The corner part of the electric potential distribution of the simulation can be seen in figure 11(a). The results shown in figures 11(b) and (c) demonstrate that the electric field distributions of both methods are similar. The 2D

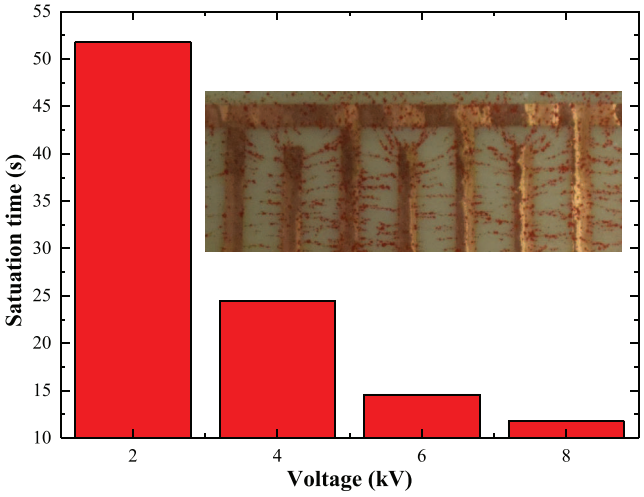

Figure 12. Relationship between the applied voltage and particle settlement time.

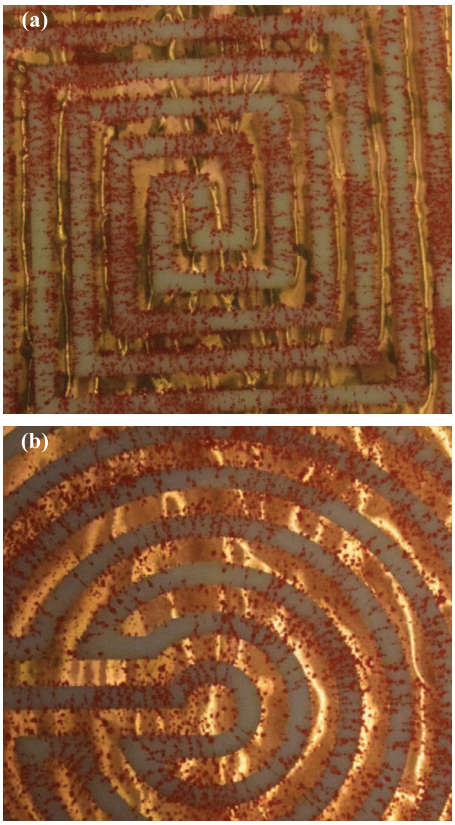

Figure 13. Indication of the electric field distribution of different pad geometries: (a) a sectional spiral pad and (b) a sectional concentric pad.

COMSOL electrostatic simulation, however, is limited in its ability to simulate the dynamic process.

Different voltages (2, 4, 6, and 8 kV) have been applied to the pad. It can be seen in figure 12 that faster response times (from turning on the power until the settlement of the particles) have been obtained with increased voltages. Also, stronger movement of the oil/semolina mixture can be seen with higher voltages. Please note that this test was captured by a 50 fps Nikon D3300 SLR camera.

This direct field visualisation method can be used to verify the indicated electric field distribution of different pad geometries, examples of which can be seen in figure 13, where a sectional spiral and concentric pad were demonstrated. It must be noted that this method, however cannot enable people to fully appreciate the dynamic discharging phase of the elector-adhesive phenomenon as the viscous nature of the oil damps the response of the particles movement in both charging and discharging. It is in the relaxation phase where the force on the particles is weaker where the experiment will be most affected by the viscosity of the medium. The particles may maintain their positions after turning off the power to the pad.

4. Conclusion and future work

The work presented in this paper has focused upon presenting two field visualization methods for understanding the dynamic electroadhesion phenomenon based on an indirect and direct experimental approach. This understanding may aid the future optimized design of electroadhesive end effectors for material handling applications. The key findings from this work are as follows:

- Visualization of the dynamic field distribution of electroadhesive pads can be indirect based on measuring surface potentials on the surface of an electroadhesive pad by an electrostatic voltmeter and direct based on charging and discharging the electroadhesive pad in a viscous oil mixed with lightweight solid particles.
- Both the indirect and direct experimental approaches presented in this paper are useful methods to understand the dynamic electroadhesion phenomenon and aid the complicated geometric optimization of electroadhesive pads based on field distributions. In addition, both methods are useful for demonstrators or lecturers to showcase or teach the dynamic electroadhesion phenomenon.
- The indirect approach can also be used to verify the condition of an electroadhesive pad before its usage. Unexpected results will occur if the pad is broken due to material degradation and under long time high voltage polarizations.

Future work of interest that will be published in future has been identified as:

- Measuring more profiles on the pad surface to obtain a more comprehensive surface potential distribution of the pad.
- Testing different pad designs and comparing their field distributions including both the charging and discharging process.
- Modelling the dynamic electroadhesion phenomenon based on the results from the indirect and direct field visualization methods.

Acknowledgments

The authors acknowledge support from the EPSRC Centre for Innovative Manufacturing in Intelligent Automation, in undertaking this research work under grant reference number EP/IO33467/1. Also, the authors acknowledge support from the Innovate UK for this work under project reference 101549.

References

[1] Krape R P 1968 *Applications Study of Electroadhesive Devices* (*NASA Contractor Report: NASA CR-1211*) (Washington, DC: National Aeronautics and Space Administration)
[2] Rahbek K 1932 Electroadhesion apparatus *Patent* US2025123 (www.google.co.uk/patents/US2025123)
[3] Prahlad H, Pelrine R, Stanford S, Marlow J and Kornbluh R 2008 Electroadhesive robots-wall climbing robots enabled by a novel, robust, and electrically controllable adhesion technology *IEEE Int. Conf. on Robotics and Automation (California, USA, 19–23 May 2008)* pp 3028–33
[4] Guo J, Tailor M, Bamber T, Chamberlain M, Justham L and Jackson M 2016 Investigation of relationship between interfacial electroadhesive force and surface texture *J. Phys. D.: Appl. Phys.* **49** 35303
[5] http://grabitinc.com/
[6] Guo J, Justham L, Jackson M and Parkin R 2015 A concept selection method for designing climbing robots *Key Eng. Mater.* **649** 22–9
[7] Graule M, Chirarattananon P, Fuller S, Jafferis N, Ma K, Spenko M, Kornbluh R and Wood R 2016 Perching and takeoff of a robotic insect on overhangs using switchable electrostatic adhesion *Science* **352** 978–82
[8] Guo J, Bamber T, Chamberlain M, Justham L and Jackson M 2017 Towards adaptive and intelligent electroadhesives for robotic material handling *IEEE Robot. Autom. Lett.* **2** 538–45
[9] Guo J, Bamber T, Chamberlain M, Justham L and Jackson M 2016 Optimization and experimental verification of coplanar interdigital electroadhesives *J. Phys. D.: Appl. Phys.* **49** 415304
[10] Ruffatto D, Shah J and Spenko M 2014 Increasing the adhesion force of electrostatic adhesives using optimized electrode geometry and a novel manufacturing process *J. Electrostat.* **72** 147–55
[11] Guo J, Bamber T, Pezting J, Justham L and Jackson M 2017 Experimental study of relationship between interfacial electroadhesive force and applied voltage for different substrate materials *Appl. Phys. Lett.* **110** 051602
[12] Brecher C, Emonts M, Ozolin B and Schares R 2013 Handling of preforms and prepregs for mass production of composites *19th Int. Conf. on Composite Materials (Montreal, Canada, 28 July–2 August 2013)* pp 4085–93
[13] Liu R, Chen R and Shen H 2013 Modeling and analysis of electric field and electrostatic adhesion force generated by interdigital electrodes for wall climbing robots *IEEE Int. Conf. on Intelligent Robots and Systems (Tokyo, Japan, 3–7 November 2013)* pp 2327–32
[14] Lin T, Rubinstein S M, Korchev A and Weitz D 2014 Pattern formation of charged particles in an electric field *Langmuir* **30** 12119–23
[15] Green N, Ramos A and Morgan H 2000 Ac electrokinetics: a survey of sub-micrometre particle dynamics *J. Phys. D: Appl. Phys.* **33** 632
[16] www.trekinc.com/products/341B.asp
[17] http://docs-europe.electrocomponents.com/webdocs/14df/0900766b814df83d.pdf
[18] Guo J, Bamber T, Hovell T, Chamberlain M, Justham L and Jackson M 2016 Geometric optimisation of electroadhesive actuators based on 3D electrostatic simulation and its experimental verification *IFAC Papers Online* **49** 309–15